SURFACE DEFECTS DETECTION ON ROLLED STEEL STRIPS BY GABOR FILTERS

Roberto Medina, Fernando Gayubo, Luis M. González, David Olmedo
CARTIF Foundation, Boecillo (Valladolid, Spain

Jaime Gómez, Eduardo Zalama, José R. Perán
ETSII, University of Valladolid, Valladolid, Spain

Keywords: Machine vision, surface inspection, defect detection, thresholding, Gabor filters.

Abstract: Product material integrity and surface appearance, in steel flat products manufacturing and processing, are important attributes that will affect product operation, reliability and customer confidence. Automated visual inspection has to be envisaged, but five major problems have to be overcome: (i) The variable nature of the defects, (ii) The high reflective nature of the metallic surfaces, (iii) The oil presence, (iv) The huge amount of visual data to be acquired and processed, and (v) The high speed in the section where inspections are performed. We have developed an automated cellular visual inspection system of flat products in a flat steel cutting factory. Among the approaches that the system uses to detect defects, we have included the two-dimensional Gabor filters. In this paper a detection procedure of defects in flat steel products based on Gabor filters is presented. The traditional methods based on the study of the grey-level histogram and shape analysis, have shown quite good results, but there are not good enough to achieve the level of success required. Experimental results show that a greater number of defects can be readily detected using the proposed approach.

1 INTRODUCTION

The steel coils produced by the iron and steel industry are rarely directly usable by the end users. Therefore, they must be reprocessed in cutting lines or processes to more manageable products with dimensions and features that the customer desires, but always with the highest quality.

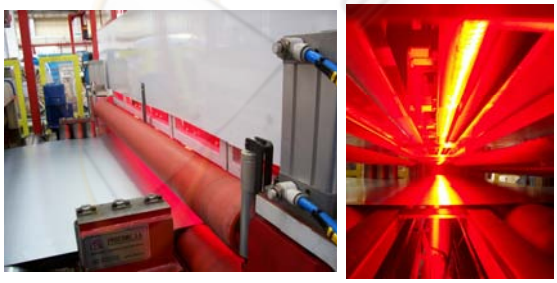

Figure 1: Automatic surface defect visual inspection system developed by CARTIF Foundation for GONVARRI Industrial (Spain).

Automated visual inspection is the obvious alternative to the human inspector (Gayubo *et al.*, 2006a; Gayubo *et al*, 2006b). An automatic surface inspection system provides the following advantages (Obeso *et al*., 1997):

- Uniform quality control.
- Programmable quality control oriented to different acceptance levels for different standards.
- Possibility of assigning different quality products to different customers, based on their requirements.

We have developed an automated cellular visual inspection system of flat products in a flat steel cutting factory (Figures 1 and 2). Among the approaches that the system uses to detect defects, we have included the two-dimensional Gabor filters. In this work a detection procedure of defects in flat steel products based on Gabor filters is presented.

Medina R., Gayubo F., González L., Olmedo D., Gómez J., Zalama E. and Péran J. (2008).
SURFACE DEFECTS DETECTION ON ROLLED STEEL STRIPS BY GABOR FILTERS.
In *Proceedings of the Third International Conference on Computer Vision Theory and Applications*, pages 479-485
DOI: 10.5220/0001088504790485

Figure 2: User interface.

Automated visual inspection has to be envisaged, but five major problems have to be overcome: (i) The variable nature of the defects, (ii) The high reflective nature of the metallic surfaces, (iii) The oil presence, (iv) The huge amount of visual data to be acquired and processed, and (v) The high speed in the section where inspections are performed (Fig. 3).

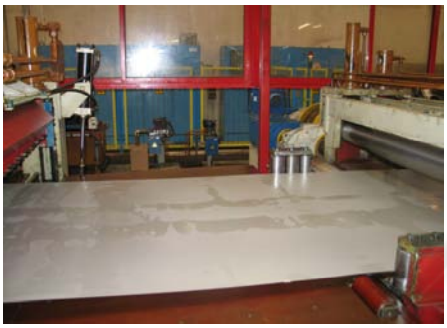

Figure 3: Coil slitting line (images courtesy of GONVARRI Group).

The practice of detecting, analysing and classifying abnormal structures in a surface is called surface inspection (Chin, 1992). Deviations form the surrounding surface can be either design elements that must have been adequately fabricated or fabrications faults that ought not have been present. It is clear the immediate detection of surface defects is important.

The number of surface defect types is large. Also the naming of similar defect may differ from plant to plant. Figure 4 shows examples of defect images.

One of the main problems of this application is the huge amount of visual data to be acquired and processed. The development of electronics and information technology have made the actual image applications possible. However the on-line inspection is not an easy task due to the subtle characteristics of the defects, high reflective nature of the metallic surfaces, and the oil presence.

A surface of flat steel products may be defined in terms of shape and reflectance, a defect may be described as a local aberration in shape and/or reflectance. The key is the ability to determine a deviation in the expected shape and reflectance of the surface.

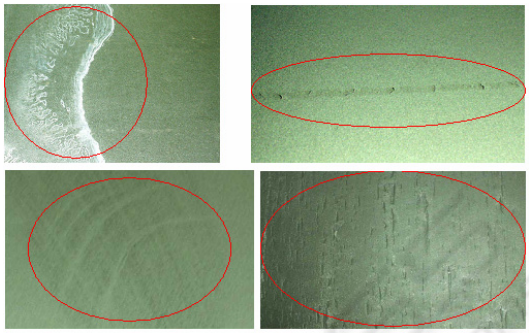

Figure 4: Surface defects. Pattern-type and roughness-type surface defects (rust, coat-less...).

Among the approaches that the system uses to detect defects, we have included the two-dimensional Gabor filters (Fig. 5). A two-dimensional Gabor filter consists of a sinusoidal wave modulated by a gaussian envelope. It performs a localized and oriented frequency analysis of a two-dimensional signal (Kamarainen, 2003). Experimental results show that a number of defects can be readily detected using the proposed approach.

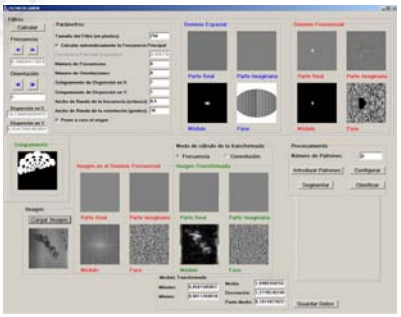

Figure 5: 2D-Gabor filters interface.

2 DEFECT DETECTION

2.1 Introduction

Many methods have been proposed to extract features either directly from the spatial domain or from the spatial-frequency domain. In the spatial domain, the more simple features are first-order statistics such as mean, variance, skewness and kurtosis from the grey-level histogram (Fig. 6) of an image (Ramana and Ramamoorthy, 1996).

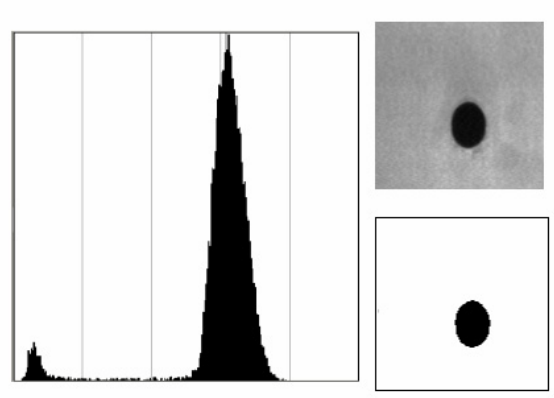

Figure 6: Thresholding.

Thresholding is a very fast and simple method, but there are two major problems. First, it is often difficult to determine, automatically or even manually, the optimal threshold. Second, only in very simple images can a threshold segment all objects correctly. To perform local thresholding, an approach is to divide the image into square sub-regions and calculate the threshold independently for each one. However, there may be some discontinuities between edges of different regions. To determinate the threshold there are two methods: consider it equal to the mean minus three standard deviations or choose the threshold according to the valley points and inflexion points of the histogram (Sahoo *et al.*, 1988).

Many work suggested that it may be possible to find better features, which are less sensitive to noise and intensity variation, in the spatial-frequency domain than those features extracted from the spatial domain (Wechsler, 1980). Measures of the shape of the spatial frequency spectrum such as location, size, and orientation of peaks in regions of spatial frequency using the 2D Fourier transform can be used to design the textural features.

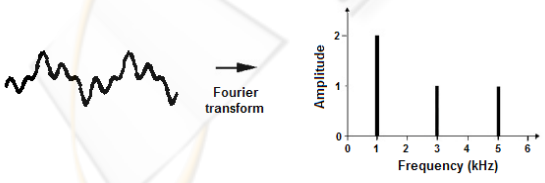

Figure 7: Fourier transform of a signal.

The Fourier methods characterise the spatial-frequency distribution, but they do not consider the information in the spatial domain. In the recent past, Gabor filters have been well recognised as a joint spatial/spatial-frequency representation for analysing images containing highly specific frequency and orientation characteristics. Daugman (Daugman, 2002) showed that Gabor filters have optimal joint localisation in both the spatial and the spatial-frequency domains. In addition, they are bandpass filters, which are inspired by a multichannel filtering theory for processing visual information in the early stages of the human visual system (Beck *et al.*, 1986).

2.2 2D Gabor Filters Bank

A two-dimensional Gabor filter consists of a sinusoidal wave modulated by a gaussian envelope. It performs a localized and oriented frequency analysis of a two-dimensional signal. The formulation in the spatial domain is the following:

$$G_{\sigma,F,\vartheta}(x,y) = g_\sigma(x,y)\cdot\exp\left[j2\pi Fx'\right]$$

$$\text{where}\quad g_\sigma(x,y) = \frac{1}{2\pi\sigma_x\sigma_y}\exp\left[-\frac{1}{2}\left(\left(\frac{x'}{\sigma_x}\right)^2+\left(\frac{y'}{\sigma_y}\right)^2\right)\right] \qquad (1)$$

$$\text{with}\quad x' = x\cos\theta + y\sin\theta \quad y' = -x\sin\theta + y\cos\theta$$

where F is the central frequency of the filter, θ is the angle between the direction of the sinusoidal wave and the x axis of the spatial domain, σ_x and σ_y the standard deviations of the gaussian envelope respectively in the direction of the wave and orthogonal to it. These last two parameters (sometimes referred to as the smoothing parameters) represent the shape factor of the gaussian surface: they determine the greater or less selectivity of the filter in the spatial domain (Fig. 8). In the above formulation it is assumed that the angle between the wave direction and the axis of the gaussian envelope is zero

Figure 8: Real part, imaginary part, magnitude and phase of Gabor filter in the spatial domain. F=0.09375; θ=0º; σx=6; σy=10.

In frequency domain the Gabor filter can be written as follows (Fig. 9):

$$G_{\sigma,F,\theta}(u,v) = \exp\left[\frac{-1}{2}\left(\frac{(u'-F)^2}{\sigma_u^2}+\frac{v'^2}{\sigma_v^2}\right)\right]$$

$$\text{where}\quad \sigma_u = \frac{1}{2\pi\sigma_x}\quad,\quad \sigma_v = \frac{1}{2\pi\sigma_y} \qquad (2)$$

$$\text{with}\quad u' = u\cos\theta + v\sin\theta \quad y \quad v' = -u\sin\theta + v\cos\theta$$

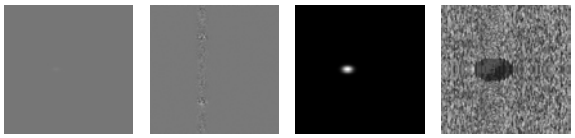

Figure 9: Real part, imaginary part, magnitude and phase of Gabor filter in the frequency domain. F=0.09375; θ=0º; σ_x=6; σ_y=10.

Gabor filters seem to have important relations with the vision system of mammals. It has been shown that the response of cortical simple cells devoted to the processing of visual signal can be approximated with Gabor functions (Daugman, 1985).

A defect detection procedure based on Gabor filters is usually carried out through the following steps:

1. design of a filter bank with filters at different frequencies and orientations;
2. computation of the transformed images;
3. extraction of a set of synthetic parameters (features) from the transformed images (definition of the feature space);
4. definition of a proper distance in the feature space;
5. detection through a suitable pattern detection algorithm.

The design of the filter bank consists in the selection of a proper set of values for the filter parameters: *F*, *θ*, *σx* and *σy*. The possible combinations of the various parameters determine how the filter bank analyses the spatial and frequency domain. In frequency domain it is common practice to display the zones covered by the various filters by plotting the half-peak magnitude iso-curves, as shown in the figure 10.

Figure 10: Half-peak iso-curve of the filter.

The design of a proper Gabor filter bank is a key aspect of the problem, and it is also controversial. Various authors proposed different values of the parameters, based on mathematical and physiological considerations. In order to simplify the selection the Gabor filter bank, we made the following assumptions: uniform separation in orientation; constant ratio between the central frequency of two adjacent filters:

- the central frequency of the filter at the highest frequency F_M
- the total number of frequencies n_F
- the total number of orientations n_O
- the ratio between the central frequencies of two adjacent filters k_F
- the value of the parameters σ_x and σ_y.

In general the highest central frequency of the filter at the highest frequency is chosen such as that the half-peak iso-curve of the filter reaches the value of 0.5, which represents the Nyquist frequency. Setting G(u,v) = 1/2 in (2), it gives the equation of the half-peak magnitude iso-curve:

$$\frac{2\pi^2\sigma_x^2}{\ln 2}(u'-F)^2+\frac{2\pi^2\sigma_y^2}{\ln 2}v'^2=1 \qquad (3)$$

This is an ellipse of semiaxes

$$a=\frac{\sqrt{\ln 2}}{\sqrt{2}\pi\sigma_x} \quad b=\frac{\sqrt{\ln 2}}{\sqrt{2}\pi\sigma_y} \qquad (4)$$

The maximum frequency value reached by the half-peak magnitude iso-curve of the filter at the highest frequency (F_M) is:

$$F_{\max}=F_M+\frac{\sqrt{\ln 2}}{\sqrt{2}\pi\sigma_x} \qquad (5)$$

Setting F_{max} = ½

$$F_M=\frac{\pi\sigma_x-\sqrt{2\ln 2}}{2\pi\sigma_x} \qquad (6)$$

The smoothing parameters, σ_x and σ_y, can be set of such way that the half peak magnitude iso-curve overlaps in greater or smaller measurement modifying in (7) the parameters K_x and K_y, called radial overlap and circumferencial overlap. Setting this values to one makes adjacent filters touch each other.

$$\sigma_x=K_x\frac{\sqrt{\ln 2}\left(2^{B_F}+1\right)}{\sqrt{2}\pi F\left(2^{B_F}-1\right)} \quad \sigma_y=K_y\frac{\sqrt{\ln 2}}{\sqrt{2}\pi F\tan\left(B_\vartheta/2\right)} \qquad (7)$$

being B_F and B_θ the frequency and orientation bandwitch, in octaves and radians respectively. The central frequency is affected by the value of σx, so the central frequency must be calculated as in (8).

$$F_M=\frac{K_x\left(2^{B_F}+1\right)}{2\cdot\left(2^{B_F}\left(K_x+1\right)+\left(K_x-1\right)\right)} \qquad (8)$$

So, first of all, we must set the radial overlap value and the frequency bandwitch, and then we calculate de central frequency and smoothing parameters.

To compute the transformed images we have used the Convolution theorem, which says that the Fourier transform of a convolution is the point-wise product of Fourier transforms:

$$f(x,y)\otimes g(x,y)=\Im^{-1}\left(F(u,v)G(u,v)\right) \qquad (9)$$

There are several features of the filter response we could measure. We could use the real part, the imaginary part, the magnitude or the phase. We have chosen the magnitude because it contains more information and it is more robust.

The detection method used is based on the concept of distance, as a measure of closeness of two points in the feature space. There several methods to measure the distance. The type of distance we adopted is called euclidean distance and can be calculated as follows:

$$\delta_{rs} = \frac{1}{N}\sqrt{\sum_{i=1}^{N}(x_{ri} - x_{si})^2} \qquad (10)$$

x_r and x_s represent two generic points in the feature space of dimension N.

2.3 Implementation

The main objective of defect detection is to determinate if there is a defect inside an image. To carry out this objective we have divide the images into two groups: defected and non-defected images, and evaluate the response of the filters.

The number of frequencies selected is eight and the number of orientations is also eight, so the filter bank is composed of 64 Gabor filters. We have adopted the approach to design the filter such as the half-peak magnitude iso-curves of adjacent filters touch each other and these iso-curves reaches the value 0,5 at the highest frequency. The size of then filter is 256x256, so the images acquired must be divided into pieces of the same size. The frequency bandwidth selected is ½ octaves. The tests carried out show us that these parameters reach the compromise between selectivity and dispersion.

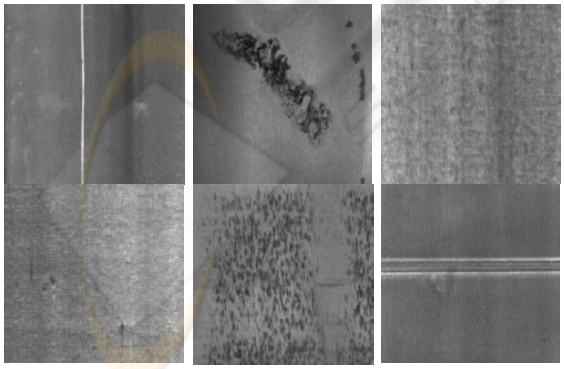

Figure 11: Defects types used in this paper.

In each image without defect we have calculated the mean value response of each of the filters of the bank. Then we have calculated the euclidean distance between the mean value calculated and the maximum value reached in every image use for training. The defected images will have a higher response to some filters in some part of the image than the images without defects.

Establishing an appropriate limit between images that contain defects and images with no defect we can achieve our goal.

3 EXPERIMENTAL RESULTS

We have studied six types of the defects commonly found in rolled steel: vertical scratch, rust, coat-less, indents, settlement marks and weld (Fig. 11).

A total of 768 images were selected for training and another 768 were used for testing. In both of the groups half of the images contain a defect and in the other half there was no defect. We have 64 images of each type of defect resulting a total of 384 images contain a defect in each group.

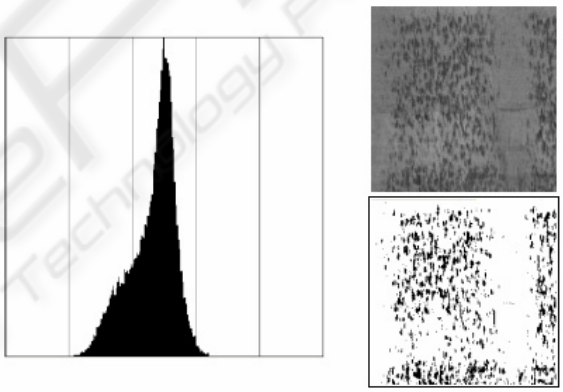

Figure 12: Segmentation based on the histogram for a settlement mark defect.

The method used in segmentation of the images is based in the idea that different objects or regions in the image have significantly different grey levels. Thresholds are usually determined from the grey-level histogram of an image. We have search for two thresholds, the upper and the lower, assuming that the zone of the image with no defect has a medium grey level. We have calculated the mean and standard deviation of the number of pixel outside the thresholds (Fig. 12).

Table 1: Mean and standard deviation of the percentage of pixel outside the thresholds.

	Mean	Standard Deviation	Percentage of detection
No defect	0.195165	0.081513	95.3125
Defect	3.131472	2.639977	91.9270
Vertical scratch	2.340807	0.174513	97.6562
Rust	5.254671	4,546847	98.8281
Coat-less	0.264038	0.091215	78.5156
Indents	0.484261	0.146349	91,4062
Settlement marks	8.31251	2.541135	86.3281
Weld	2.132541	0.419870	98.8281

As we can see in the chart above (Table 1), there are a 4.69 rate of false positives, and the defects are correctly detected in 91.93%.

To improve the results obtained with the grey-level histogram we have developed the Gabor filter. Observing the response of the these filters for training images (Fig.13), we have established the limit that separate the defect images and the no defect images. The test images have been used to determinate the goodness of the method.

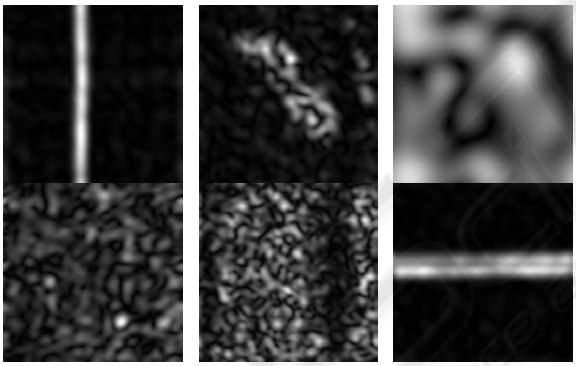

Figure 13: Some transformed images used in this paper.

Table 2: Mean and standard deviation of the euclidean distance.

	Mean	Standard Deviation	Percentage of detection
No defect	0.158103	0.035414	99.21875
Defect	0.375900	0.101831	96.61458
Vertical scratch	0.395899	0.076832	97.6562
Rust	0.353493	0.130730	85.9375
Coat-less	0.264038	0.010007	98.82812
Indents	0.374794	0.046349	99.21875
Settlement marks	0.407765	0.068066	98.82812
Weld	0.459415	0.075339	99.21875

The measure of the distance can be observed in the next chart (Table 2). We can see in this chart the mean value and the standard deviation of the euclidean distance between the mean value, obtained with the training images without defect, and the maximum value of then transformed image. In the third column we can see the percentage of defect detection obtained with the testing images. The first two rows show the results for no-defect and defect images. The rest of the rows show the results for each type of defect studied.

We can see that we detect 96,61% of the defects, obtaining only a 0,78% of false positives. The defect of rust is the one that reaches the worst results, obtained almost 86% of right detection. The rest of defects are detected around 99%.

4 CONCLUSIONS

Quality control is a key process in steel flat products manufacturing and processing. Coil slitting and cutting is a paradigmatic process: often 200 meters a minute process speed is reached, so than human visual inspection is dramatically restricted.

We have developed an automated cellular visual inspection system of flat products in a flat steel cutting factory (GONVARRI Burgos, Spain). Among the approaches that the system uses to detect defects, we have included the traditional methods and two-dimensional Gabor filters.

The traditional methods based on the study of the grey-level histogram and shape analysis, have shown quite good results, but there are not good enough to achieve the level of success required. It has been necessary the implementation of new methods. The application of Gabor filters seem to be a good alternative to the traditional methods.

The results obtained in the detection of six of the most common defects that appear over the surface of the steel have reached a rate of 96,61% of right detection, obtaining only a 0,78% of false positives.

ACKNOWLEDGEMENTS

This research is partially funded by GONVARRI Group, the Spanish FIT-020400-2006-125 research project, and the Agencia de Inversiones y Servicios (ADE) of Castilla y León (Spain).

REFERENCES

Beck, J., Sutter, A. and Ivry, R., 1987. Spatial frequency channels and perceptual grouping in texture segregation . *Computer Vision. Graphics and Image Processing*. pp. 299–325.

Chin, R.T., 1992. Automated visual inspection algorihms. In: Computer Vision: Theory and Insdustrial Applications, *Springer Verlag*, New York, pp. 377-404.

Daugman, J.G., 1985. Uncertainty relation for resolution in space, spatial frequency, and orientation optimized by two-dimensional visual cortical filters, *J. Opt. Soc. Am*., vol. 2, pp. 1160-1169.

Daugman, J.G., 2002. Gabor wavelets and statistical pattern recognition. *The Handbook of Brain Theory and Neural Networks.* 2nd ed.. MIT Press (M. Arbib. editor). pp. 457-463.

Gayubo, F., González, J.L., de la Fuente, E., Miguel, F., and Perán, J.R., 2006. On-line machine vision system for detect split defects in sheet-metal forming processes. *Conference on Pattern Recognition. ICPR 2006.* vol. 1, pp. 723-726.

Gayubo F., González L.M., Olmedo D., Medina R. Goméz J., González J.L. 2006. Inspección visual en línea de defectos en piezas de chapa embutida. *Proc. XVI Congreso de Máquinas-Herramienta y Tecnologías de Fabricación*. vol. 1. pp. 715-728.

Hubel, D.H. and Wiesel, T.N., 1962. Receptive fields, binocular interaction, and functional architecture in the cat's visual cortex *J Physiol*. (Lond.), vol. 160, pp. 106-154.

Kamarainen, J.K., 2003. Feature extraction using Gabor filters. *PhD thesis*.

Obeso, F., Gonzalez, J.A., Dominguez, S., Campoy, P. and Mochon, J., 1997. Intelligent on-line surface inspection on a skinpass mill. *Iron and Steel Engineer*.

Parker, J.R., 1997. Algorithms for Image Processing and Computer Vision. *Wiley Computer Publishing*.

Phan, D.T. and Alcock, R.J., 2003. *Smart Inspection Systems. Techniques and applications if Intelligent Vision.* Ed. Academic Press.

Porat, M. and Zeevi, Y.Y., 1988. The generalized Gabor scheme of image representation in biological and machine vision. *IEEE Transactions on Pattern Analysis Machine Intelligence*. pp. 452–468.

Ramana, K.V. and Ramamoorthy, B., 1996. Statistical methods to compare the texture features of machined surfaces. In: *Pattern Recognition*. pp. 1447–1459.

Sahoo P.K., Soltani S., Wong, A.K.C. and Chen Y.C., 1988. A Survey of Threshonding Techniques. *Computer Vision, Graphics and Image Processing.* Vol. 41, pp. 233-260.

Tsai, D.M. and Wu, S.K., 2000. Automated Surface Inspection Using Gabor Filters *Int J Adv Manuf Technol.* pp. 474–482.

Wechsler, H., 1980. Texture analysis: a survey. *Signal Processing*. pp. 271–282.